7 minutes past geometric occultation, that is, down to 40-km altitude, the X-band signal fades rapidly and is completely gone before reaching 51 km.

Figure 6 shows the pressure obtained from the DSS 12 measurements plotted on a logarithmic scale as a function of temperature. Superimposed upon this profile, marked by triangles, are pressure and temperature measurements from the Soviet probe, Venera 8 (*21*). Although in general the two profiles are similar, there are significant variations. The most likely explanation for this deviation is the assumption of the pure carbon dioxide composition, although the uncertainties in the Venera 8 measurements (± 1.5 percent of full scale) could also contribute to the discrepancy.

Ionosphere. Open-loop receiver differential Doppler data were used to measure the nightside and dayside ionospheres of Venus. Mariner 5 423.3-Mhz amplitude data (*3*) showed a peak density of approximately 2×10^4 electron/cm^3 near an altitude of 142 km on the night side. It was not possible from those data to produce a reliable estimate of the electron number density distribution below that altitude, for it was unclear whether the observed amplitude changes were due to spherical stratification or to scintillation effects caused by horizontal irregularities.

The Mariner 10 data revealed two peaks as shown in Fig. 7, labeled "night." The upper one is located at 140 km and has a peak density of approximately 10^4 electron/cm^3. A second peak with slightly lower density was observed at 120-km altitude. It is clear from both the closed- and open-loop differential Doppler data that these are thin, well-defined layers. The peak density obtained is in good agreement with that obtained from the Mariner 5 experiment where the immersion point was 30° farther north in latitude.

The dayside profile is also shown in Fig. 7. A peak number density of 3×10^5 electron/cm^3 was observed near 145-km altitude. The Mariner 5 dual-frequency experiment, which was more sensitive to tenuous plasmas as a result of the use of lower frequencies, indicated that an ionopause existed near 500-km altitude on the day side. The Mariner 10 differential Doppler data show a similar effect near 530 km. The density change, however, is only 10^3 electron/cm^3 across the ionopause boundary instead of the 10^4 electron/cm^3 seen by Mariner 5. This is very close to the S-X system noise level at this stage in processing the data and, therefore, may not be real.

H. T. HOWARD, G. L. TYLER
Center for Radar Astronomy, Stanford University, Stanford, California 94305
G. FJELDBO, A. J. KLIORE
G. S. LEVY, D. L. BRUNN
R. DICKINSON, R. E. EDELSON
W. L. MARTIN, R. B. POSTAL
B. SEIDEL, T. T. SESPLAUKIS
D. L. SHIRLEY, C. T. STELZRIED
D. N. SWEETNAM, A. I. ZYGIELBAUM
Jet Propulsion Laboratory, California Institute of Technology, Pasadena
P. B. ESPOSITO, J. D. ANDERSON
Jet Propulsion Laboratory
I. I. SHAPIRO, R. D. REASENBERG
Department of Earth and Planetary Sciences, Massachusetts Institute of Technology, Cambridge 02139

References and Notes

1. G. Fjeldbo and V. R. Eshleman, *Planet. Space Sci.* **16**, 1035 (1968); A. J. Kliore, D. L. Cain, G. Fjeldbo, B. L. Seidel, M. J. Sykes, S. I. Rasool, *Icarus* **17**, 484 (1972).
2. R. L. Koehler, *J. Geophys. Res.* **73**, 4883 (1968).
3. Mariner Stanford Group, *Science* **158**, 1678 (1967).
4. J. A. Dunne, *ibid.* **183**, 1289 (1974).
5. J. D. Anderson and L. Efron, *Bull. Am. Astron. Soc.* **1**, 231 (1969).
6. P. Goldreich and S. J. Peale, *Astron. J.* **72**, 662 (1967); E. Bellomo, G. Colombo, I. I. Shapiro, in *Mantles of the Earth and Terrestrial Planets*, S. K. Runcorn, Ed. (Interscience, London, 1967), p. 193.
7. See, for examples, I. I. Shapiro [*Science* **157**, 423 (1967)], R. L. Carpenter [*Astron. J.* **75**, 61 (1970)], and R. F. Jurgens [*Radio Sci.* **5**, 435 (1970)]. Whether the small differences between these determinations and the resonance value are significant has not yet been well determined; none is more than three times the estimated standard error.
8. The averaging times for the Doppler data varied from 10 to 300 seconds.
9. The corresponding value for the product of Venus's mass and the gravitational constant is 324,858.6 ± 1.0 km^3/sec^2.
10. Estimates of the second-degree unnormalized coefficient, J_2, vary between 10^{-6} and 2×10^{-5}, and the longitudinal harmonics (C_{22} and S_{22}) fall within the range 10^{-6} to 10^{-5}. The definition of the spherical harmonic expansion of the gravitational potential is given in W. M. Kaula, *Theory of Satellite Geodesy* (Blaisdell, New York, 1966).
11. The root-mean-square value represents about 2 parts in 10^8 of the measured Doppler shift and about 6 parts in 10^8 of the change in Doppler shift during the day of encounter.
12. I. I. Shapiro, G. H. Pettengill, G. N. Sherman, A. E. E. Rogers, R. P. Ingalls, *Science* **179**, 473 (1973).
13. A. J. Kliore, in *NASA TM X-62,150* (L. Colin, Ed.) (1972), sect. 3, pp. 2–16.
14. M. E. Ash, D. B. Campbell, R. B. Dyce, R. P. Ingalls, R. Jurgens, G. H. Pettengill, I. I. Shapiro, M. A. Slade, W. B. Smith, T. W. Thompson, *Science* **160**, 985 (1968).
15. W. G. Melbourne, D. O. Muhleman, D. A. O'Handley, *ibid.*, p. 987.
16. J. D. Anderson, D. L. Cain, L. Efron, R. M. Goldstein, W. G. Melbourne, D. A. O'Handley, G. E. Pease, R. C. Tausworthe, *J. Atmos. Sci.* **25**, 1171 (1968).
17. V. R. Eshleman, G. Fjeldbo, J. D. Anderson, A. Kliore, R. B. Dyce, *Science* **162**, 661 (1968).
18. G. Fjeldbo, A. J. Kliore, V. R. Eshleman, *Astron. J.* **76**, 381 (1971).
19. A. J. Kliore, D. L. Cain, G. S. Levy, G. Fjeldbo, S. I. Rasool, in *Space Research IV*, A. Dollfus, Ed. (North-Holland, Amsterdam, 1969).
20. B. C. Murray *et al.*, *Science* **183**, 1307 (1974).
21. M. Ya Marov, V. S. Avduyevskiy, N. F. Borodin, V. V. Kershanovich, V. P. Lysov, B. Ye. Moshkin, M. K. Rozhdestvenskiy, O. L. Ryabov, A. P. Ekonomov, *NASA Tech. Transl. F-14,909* (1973).
22. We thank the personnel of the Mariner Project and the Deep Space Net for their excellent support in the acquisition of data. We are particularly indebted to R. Allis, J. M. Hardman, E. R. Kelly, M. Simes, P. M. Woiceshyn, G. A. Wood, and the project navigation team. This report presents the results of one phase of research carried out at the Jet Propulsion Laboratory, California Institute of Technology, under contract No. NAS 7-100, sponsored by the National Aeronautics and Space Administration.

4 March 1974

Magnetic Field Observations near Venus: Preliminary Results from Mariner 10

Abstract. *The NASA-GSFC magnetic field experiment on Mariner 10 is the first flight of a dual magnetometer system conceived to permit accurate measurements of weak magnetic fields in space in the presence of a significant and variable spacecraft magnetic field. Results from a preliminary analysis of a limited data set are summarized in this report, which is restricted primarily to Venus encounter. A detached bow shock wave that develops as the super Alfvénic solar wind interacts with the Venusian atmosphere has been observed. However, the unique coincidence of trajectory position and interplanetary field orientation at the time of bow shock crossing led to a very disturbed shock profile with considerably enhanced upstream magnetic fluctuations. At present it is not possible to ascertain the nature and characteristics of the obstacle responsible for deflecting the solar wind flow. Far downstream disturbances associated with the solar wind wake have been observed.*

Introduction. Results from a preliminary analysis of a limited and at times low quality quick-look data set for the NASA-GSFC magnetic field experiment are summarized in this report. There appears to be sufficient evidence for an initial assessment of the results, particularly as related to the study of the solar wind interaction with Venus. What emerges is an interpretation based heavily upon our understanding of certain features of the solar wind interaction with the earth's magnetic field, although for Venus the interaction is directly with the planetary ionosphere. The experiment is unique in being the first flight of a dual magnetometer system on a spacecraft that was built without any constraints limiting the spacecraft magnetic fields. As such, the experiment has worked perfectly, achieving the objective of accurate measurements of both the weak interplanetary magnetic field during the cruise from the earth to Venus and the stronger and more variable fields associated with the encounter.

Previous studies. The first measurements of the Venusian environment were made by Mariner 2 in December 1962. At a flyby distance of 41,000 km (6.6 R_V), no disturbances of the interplanetary medium associated with the planet were identified (*1*). Subsequently, Venera 4 (*2*) and Mariner 5 (*3*) performed magnetic field and plasma measurements 1 day apart in October 1967 which clearly identified a detached bow shock wave surrounding the planet. The last spacecraft to study the plasma field environment of Venus was Venera 6, which impacted the planet in May 1969 (*4*).

None of these earlier studies provided any evidence for the existence of an intrinsic planetary magnetic field. Upper limits to the magnetic moment have decreased significantly; the lowest estimate, based upon the Venera 4 magnetic field data, was obtained when the spacecraft was 200 km from the planetary surface. This limit, a magnetic moment less than 10^{-4} of the earth's, is equivalent to a surface equatorial field strength of less than 4γ ($1\gamma = 10^{-5}$ gauss). Such a low value is insufficient to deflect the solar wind flow, as does the earth's magnetic field. Data from Mariner 10, because of its trajectory, cannot presently reduce further this upper limit to the magnetic moment of Venus.

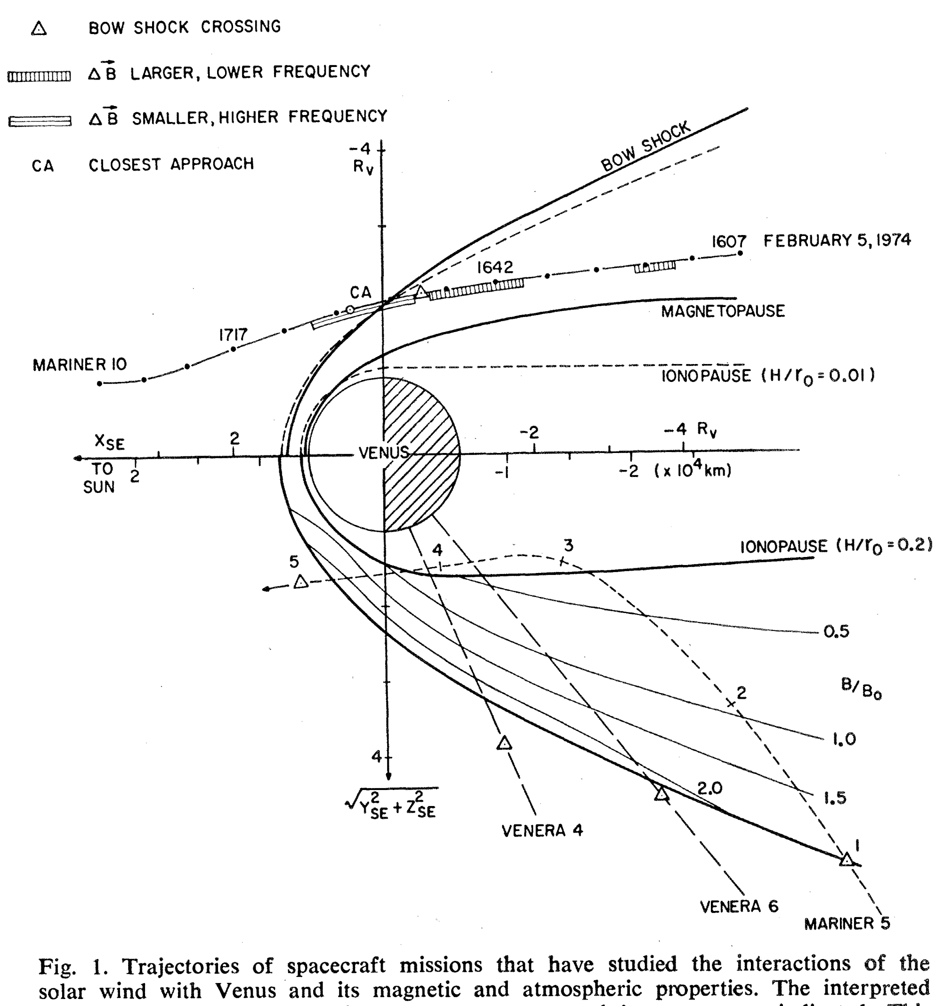

Fig. 1. Trajectories of spacecraft missions that have studied the interactions of the solar wind with Venus and its magnetic and atmospheric properties. The interpreted boundary locations of bow shock, magnetopause, and ionopause are indicated. This figure assumes cylindrical symmetry about the sun-Venus line (X_{SE}). The Y_{SE} coordinate is chosen parallel to the ecliptic. Note that the lower half of the figure refers to results before Mariner 10 while the upper half refers to interpretations in this report.

The trajectories of these spacecraft and interpretation in terms of a detached bow shock wave are shown in the lower half of Fig. 1. The coordinate system has cylindrical symmetry about the sun-Venus line, approximately the direction of solar wind flow. Although there is reasonably good agreement in the location of the bow shock, there is not a consensus regarding the nature of the obstacle responsible for the deflection of solar wind flow. Some investigators (*5*) have assumed that a direct interaction between the solar wind plasma and planetary atmosphere leads to plasma deflection. Others (*6*) have assumed the existence of a boundary surface, an ionopause, identical to a tangential discontinuity in magnetohydrodynamics separating the two immiscible plasmas of the solar wind and planetary ionosphere. Still others (*7*) have assumed a more complicated interaction, in which an induced magnetic field arises from electrical currents associated with the convecting interplanetary magnetic field embedded in the solar plasma as it flows past the planet. This leads to the development of a pseudomagnetopause. Finally, it has also been suggested that the interaction is more analogous to that of the solar wind with the rarefied atmosphere of a comet (*8*) in which an extended interaction region leads to a nearly shockless deceleration and deflection of the solar wind flow.

The magnetic field experiment during Venus encounter was performed to yield further observational detail of the detached bow shock wave surrounding Venus and to attempt to understand the nature of the obstacle to solar wind flow.

Instrumentation. The magnetic field experiment consists of two triaxial fluxgate magnetometer sensors and a moderately long boom (5.8 m) in a dual magnetometer arrangement (*9*) with the sensors separated by 2.3 m. This is done to permit analytic separation of the ambient field in space from a significant and variable spacecraft field. Magnetometer electronics provide two ranges of $\pm 16\gamma$ and $\pm 128\gamma$ for each component extended to $\pm 3188\gamma$ by bias level logic. Vector measurements of the field with ten-bit precision, yielding quantization step sizes of 0.030γ and 0.26γ in the low and high ranges, respectively, are made every 40 msec. The root mean square (RMS) noise level of each sensor over the 0- to 12.5-hertz band pass ranges between 0.03 and 0.06γ. Data from the outer magnetometer are sent directly to ground at the basic sampling rate while the inner magnetometer data are averaged over three samples (120 msec) on board the spacecraft and these averages are transmitted.

Ground data processing begins by merging the data from the two magnetometers to estimate the spacecraft magnetic field according to the formula

$$\mathbf{B}_{sc}(\text{outer}) = \frac{\alpha}{1-\alpha}[\mathbf{B}(\text{inner}) - \mathbf{B}(\text{outer})] \qquad (1)$$

where the field vectors on the right side are the measured fields at the inner and outer sensors and α is the dual magnetometer coupling coefficient determined theoretically to be 0.30 for a spacecraft-centered dipole. Preflight static magnetic mapping of the spare spacecraft plus preliminary analysis of in-flight spacecraft field variations indicate that the spacecraft field at the remote locations of the sensors is well represented by such a dipole but of variable magnitude and orientation.

Three-second averages of this estimate of the spacecraft field at the outer sensor position are then subtracted from the detailed data (25 samples per second) to yield an accurate estimate of the instantaneous ambient field according to the formula:

$$\mathbf{B}^{est}_{amb} = \mathbf{B}(\text{outer}) - \langle \mathbf{B}^{est}_{sc}(\text{outer}) \rangle \qquad (2)$$

In this analysis, the measured fields are calculated by using sensor zero-point offset values determined before flight and from in-flight data during spacecraft roll maneuver periods and from times when the outboard mechanical sensor flipper was activated. When this report was prepared, the data from only the first of four roll calibration maneuvers performed between launch and Venus encounter were available. In these preliminary data, we believe that the estimates of the ambient field are accurate to $\pm$ 1.0γ or better for each component. The nature of the observations is such that this uncertainty does not adversely influence our interpretation of data in this report. When appropriate production data tapes are received, it is expected that the accuracy will be improved to better than 0.5γ.

Figure 2 shows a plot of data obtained on 15 December 1973 in the standard format of 6-second averages of the ambient field in solar ecliptic coordinates and the associated spacecraft field at the outer magnetometer position (labeled S/C). The ambient field data are given in terms of field magnitude $\overline{F}$ (in gammas), azimuthal angle ϕ ($\phi = 0°$ toward the sun) measured counterclockwise looking down from the north ecliptic pole, and inclination angle θ relative to the ecliptic, positive northward. A reconstituted average vector magnetic field is obtained from component averages, and the RMS parameter, barely visible, represents the Pythagorean mean of the three-component RMS deviations over the same interval.

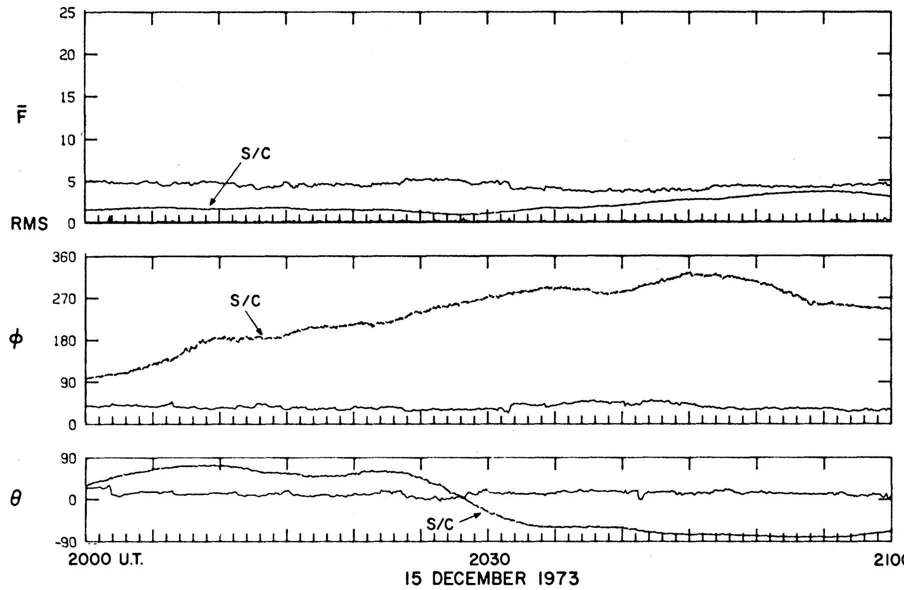

Fig. 2. Six-second averaged interplanetary magnetic field (IMF) observations of the National Aeronautics and Space Administration–Goddard Space Flight Center (NASA-GSFC) during calibration of the spacecraft television system on 15 December 1973. The plot shows variations of the spacecraft magnetic field as measured at the outboard sensor, while the IMF remains essentially constant. The coordinate system is spacecraft-centered solar ecliptic with additional definitions in the text; $\phi = 0°$ is the spacecraft-sun line; *S/C*, spacecraft.

At the time of these data, the spacecraft was approximately midway between the earth and Venus in heliocentric radial distance and about 21° leading Venus in differential heliocentric longitude. Thus the data represent observations taken well away from the influence of either the earth or Venus. The ambient field is typical of that observed in interplanetary space near 1 A.U. in magnitude and fluctuation level although ϕ is usually closer to 135° or 315°.

Activity on board the spacecraft associated with scan platform motion during the calibration of the television system causes the observed spacecraft field to change in both magnitude and direction. The magnitude of the spacecraft field at the outer sensor position varies by more than 100 percent from a typical value of 2γ to as great as 4γ on occasion. Even more important, large angular variations of the spacecraft field occur in concert with varying pointing directions of the television cameras. Such large spacecraft field variations were not expected before flight.

Venus wake and encounter observations. The trajectory of Mariner 10 before encounter is uniquely well-positioned to study the aft body pattern of solar wind flow past Venus. For more than 6 days before encounter, the spacecraft is within a cone of half-angle 15° centered on the sun-Venus line with the apex at the planet. During this time the spacecraft moves from $\sim$ 750 R_V downstream toward the planet. The magnetic field measurements are suggestive of the sporadic detection of a taillike phenomenon in which the magnetic field at times is quieter (fewer fluctuations), and slightly stronger (approximately 12γ) than usual and closely aligned with the extended sun-Venus line. It seems plausible that these intervals are associated with the solar wind wake of Venus and, as such, they would represent the downstream detection of disturbances in the interplanetary medium trailing behind the planet at scale distances greater than any other planetary wake thus far

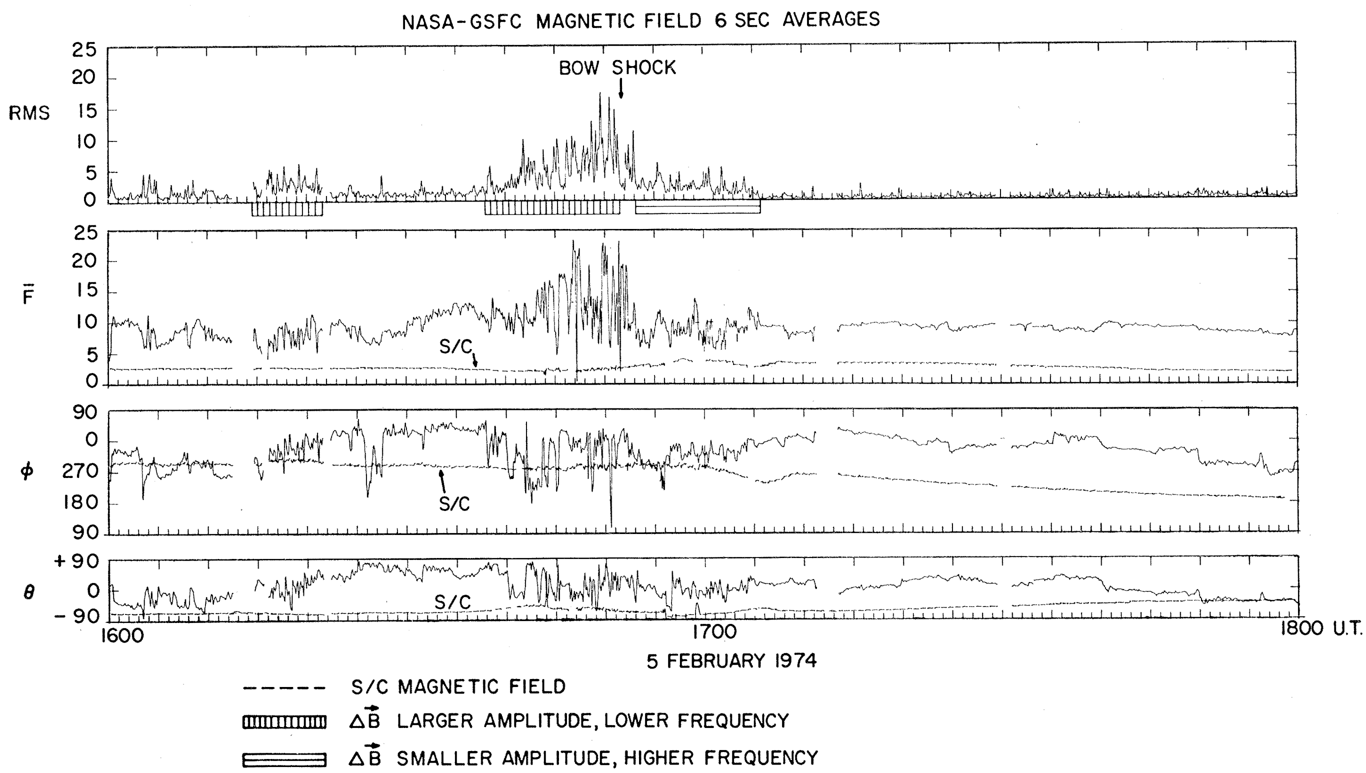

Fig. 3. NASA-GSFC 6-second averaged magnetic field data near encounter presented in spacecraft-centered solar ecliptic coordinates. Bow shock crossing occurs around 16:52 ± 1 U.T. Data gaps are due to missing or erroneous transmissions.

studied, including the notable magnetic tail wake of the earth. The observations of the earth's tail wake at 3000 R_E must be normalized by the scale size of the earth's magnetosphere (10 to 15 R_E). Thus the nondimensional downstream scale distance for the most distant observation of the terrestrial plasma tail wake is less than 300 as compared to ~ 700 for Venus. No other spacecraft mission studying any of the planetary environments has had a trajectory so well situated for the study of the downstream wake conditions as has Mariner 10 for Venus.

The data from which this interpretation was made correspond to near real time spacecraft data transmission and elementary ground processing to produce 42-second averages of the magnetic field which are replete with data dropouts and error artifacts that restrict further quantitative studies. The possibility of correlated and coherent changes of the electron plasma observations is suggested, but further analysis must await the availability of appropriate data tapes.

The portion of the trajectory near Venus which is relevant to detailed study of the solar wind interaction with the planet is shown in the top half of Fig. 1. Shortly after closest approach at 1702 U.T., the spacecraft passed into a radio occultation period during which data were stored on a spacecraft magnetic tape recorder for subsequent retransmission. Special processing at the Jet Propulsion Laboratory, Pasadena, California, has made available to us quick-look data tapes for both the real time and playback data at encounter. The three-dimensional nature of the spacecraft trajectory is such that for the interval shown, the spacecraft was initially 1.5 R_V above the solar ecliptic X-Y plane while at closest approach Z had decreased to 0.5 R_V. Upstream of the planet, the spacecraft passed below the X-Y plane as well as across the X-Z plane at 1753 U.T. when $Z = -0.8\ R_V$.

Data for the time interval from 1600 to 1800 U.T. surrounding encounter are shown in Fig. 3. Several regions having distinctly different magnetic field magnitude and fluctuation characteristics are evident. The very large amplitude fluctuations observed between 16:38:30 and 16:53:30 U.T. are interpreted as being associated with approach and immediate proximity to the bow shock, crossed at approximately 16:51:30 U.T.

The average amplitude of the magnetic field upstream from the bow shock crossing is enhanced by approximately 100 percent downstream from the shock crossing, while the RMS deviation correspondingly increases by more than a factor of 3. Although the profile or signature of this bow shock crossing is not as distinctive in characteristics as many of the classical terrestrial bow shock crossings, it is consistent with the type referred to as pulsation shock, which occurs when the orientation of the upstream magnetic field is at an angle of close to 0° with respect to the normal direction of the bow shock surface (*10*). This is referred to as a parallel shock in the nomenclature of magnetohydrodynamics.

A more revealing presentation of the magnetic field data is shown in Fig. 4, in which the detailed 40-msec measurements of the magnetic field are presented in both magnitude and two angles as well as three orthogonal components on a considerably expanded time scale. Four minutes of data surrounding the bow shock crossing are presented as well as a short interval of playback data obtained further upstream. The difference in the character of the magnetic field fluctuations is now more readily discerned. Downstream, before 16:51:30 U.T., are seen primarily large amplitude, low frequency fluctuations, while the shock crossing itself, which takes approximately 2 minutes, is associated with the onset of much higher frequency fluctuations than are observed far upstream from the bow shock until approximately 1706 U.T. The bow shock crossing is defined as beginning with the higher frequency fluctuations and terminating with the decrease of the field magnitude to approximately its upstream value.

During playback, that is, after 1707 U.T., the RMS deviation of the field is much lower than during the encounter period, and the averages show only very small deviations. Near 16 : 18 : 30 U.T., there is a small interval of data having characteristic fluctuations reminiscent of the larger amplitude fluctuations immediately preceding the bow shock crossing. As shown in Fig. 3, the spacecraft field is continuously changing in both magnitude and direction in a generally smooth manner associated with the television scan platform motion. There is also a fine-scale ripple of approximately 0.2γ in field magnitude associated with the stepper motor of the infrared radiometer experiment.

Interpretation and discussion. The two principal questions to be answered concerning the solar wind interaction with Venus are as follows: (i) Does a bow shock exist and is it similar in character to that surrounding the earth's magnetosphere if the upstream interplanetary conditions are taken into account? (ii) What is the nature of and characteristic physical parameter set describing the obstacle causing the solar wind deflection around the planet and the extended wake region trailing behind it? From the preceding short data presentation and description of magnetic field observations on Mariner 10, it appears fairly certain that a bow shock wave of pulsation type surrounding the planet was detected at approximately 1652 U.T. The change of the magnetic field and its fluctuations is not characteristic of a sharp bow shock crossing. It is more analogous to the very disturbed conditions that arise when the upstream magnetic field orientation is nearly parallel to the local bow shock normal (*10*).

This condition leads to the development of a more complex and disturbed shock structure and signature and considerably enhances the occurrence immediately upstream of magnetic field fluctuations in several separate frequency regimes (*11*). Preliminary spectral analyses are consistent with the impression obtained by visual inspection of the time domain data regarding the identification of lower frequency and higher frequency fluctuation regimes. These are noted on the trajectory and data plots of Figs. 1 and 3.

The computations show that the field fluctuations downstream occur primarily at frequencies less than approximately 1 hertz, while upstream there is considerable enhancement of fluctuations higher than 1 hertz; these extend almost 1 R_V upstream from the bow shock crossing. Thus, it is difficult to precisely determine an average magnetic field configuration in the presence of the large amplitude component fluctuations in Figs. 3 and 4. Nonetheless, throughout most of the upstream data immediately following the bow shock crossing, the field orientation is appropriate for satisfying the necessary

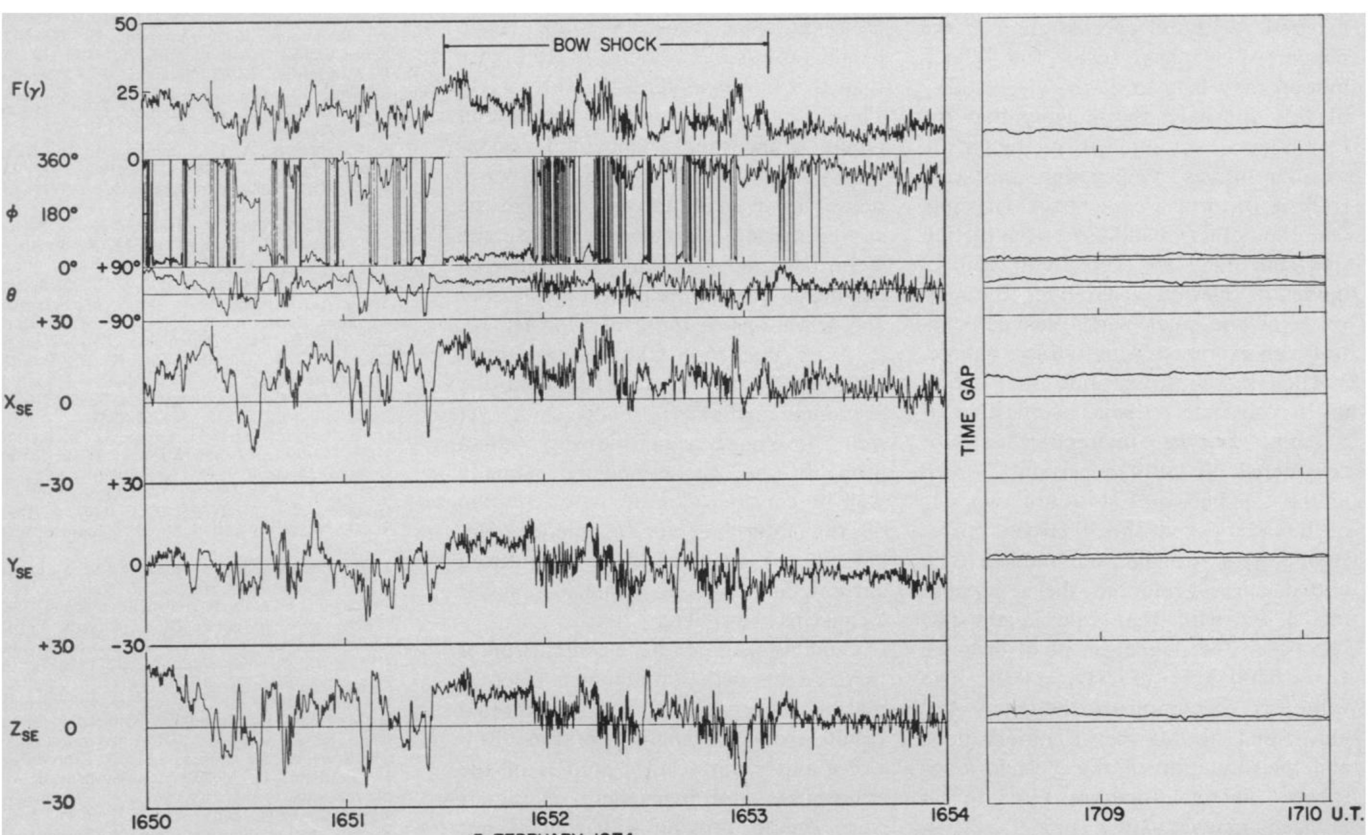

Fig. 4. NASA-GSFC detailed magnetic field data with sampling interval of 40 msec during the bow shock crossing (16:51:30 to 16:53:00 U.T.) in spacecraft-centered solar ecliptic coordinates. Data from the relatively undisturbed upstream regime from 17:08:00 to 17:09:30 U.T. are also presented.

criteria for nearly parallel shock and upstream waves. At approximately 1706 U.T., the decrease in the amplitude of the field fluctuations, readily evidenced by the RMS data in Fig. 3, suggests that the field orientation has changed such that the field line does not thread the bow shock and therefore the upstream high frequency waves are absent. It is also reasonable to assume that the waves have been attenuated as they propagate upstream, and this contributes to their absence.

The foregoing interpretation of the Venusian solar wind interaction characteristics is based heavily upon our current understanding of solar wind interaction with the earth. It is possible that the interaction region at Venus is a considerably more complex phenomenon than previously anticipated; namely, these magnetic field data may be consistent with the primitive models of the solar wind interaction with a cometary atmosphere in which the solar wind is decelerated in a broad region and a weak shock subsequently develops. Under such conditions, the position of the weak shock in the magnetic field would be expected to occur at approximately the same position as a classical magnetohydrodynamic shock. Further study of the fluctuations of the magnetic field and consideration of the possibility of large-scale bow shock motion may help to clarify the validity of this approach by showing that the fluctuations are indeed characteristic whistler waves propagating upstream from a disturbed bow shock crossing. On the other hand, the fluctuation spectrum may be consistent with a model of plasma instabilities that develop as the solar wind plasma penetrates an extended Venusian ionosphere.

The situation regarding the nature of the obstacle to solar wind flow, if a cometary-type interaction is not considered, is also uncertain. Shown in the top half of Fig. 1 are two sets of boundary and shock curves corresponding to two different models. The dotted curves refer to the ionopause model (*6*) with the scale height (H) relative to the stagnation point distance ($r_0 = 6500$ km) of $H/r_0 = 0.01$. The value for the ionopause height is 450 km, based on Mariner 5 observations and interpretation of the dayside ionosphere. The solid curves refer to an induced magnetopause model (*7*) in which the stagnation point magnetopause height is assumed to be 150 km, based upon the maximum ionospheric conductivity (and induced current flow) suggested by Mariner 5 data. Both the magnetopause and bow shock wave positions are scaled from the terrestrial case by assuming appropriate scaling factors of the terrestrial magnetosphere and the Venusian pseudomagnetosphere. Both the theoretical computation as well as the scaling of the terrestrial observations show that the bow shock position is in reasonably good agreement with the Mariner 10 observations. However, changes in the direction of solar wind flow from the sun-Venus line, due to both aberration and actual nonradial solar wind flow, could easily alter the expected position of the bow shock and bring either of the two bow shock curves into perfect agreement with observations. The position of the bow shock can also be adjusted by changing the upstream sonic and Alfvénic Mach numbers, so it is not possible, on the basis of the observed position of the Venusian bow shock, to uniquely determine which of the possible models of the obstacle to solar wind flow is the most plausible.

The lower half of Fig. 1 also includes the theoretical ionopause and bow shock positions which show good agreement with observations from Mariner 5, Venera 4, and Venera 6. However, the corresponding scale height ratio is 0.2, a factor of 20 higher than that corresponding to Mariner 10. Thus, if the appropriate interaction model is the simple tangential discontinuity equivalent boundary, the ionopause, it is possible to conclude that the compositional characteristics of the Venusian atmosphere may have changed significantly from the period of Mariner 5 observations to those of Mariner 10, in order that H would decrease from 1300 to 65 km. On the other hand, the pseudomagnetopause model, not yet well developed quantitatively, could probably be accommodated equally well by consideration of the orientation of the interplanetary magnetic field, velocity of solar wind flow, induced current, as well as a slightly modified Venusian ionosphere.

Conclusion. The future comparison of these results with simultaneous electron plasma observations and interpreted results from the analysis of the ultraviolet and radio science studies of the atmosphere and ionosphere characteristics should provide a partial if not complete resolution of the various possible interpretations. However, the detailed physical nature of the obstacle might continue to elude identification until similar high fidelity in situ measurements are made near the stagnation point at altitudes of 100 to 500 km by a probe or orbiting spacecraft.

N. F. NESS
K. W. BEHANNON
R. P. LEPPING
Goddard Space Flight Center, Greenbelt, Maryland 20771
Y. C. WHANG
Catholic University, Washington, D.C. 20017
K. H. SCHATTEN
Victoria University, Wellington, New Zealand

References and Notes

1. M. Neugebauer and C. W. Snyder, L. Frank, J. A. Van Allen, H. K. Hills, *Science* **139**, 905 (1963); *J. Geophys. Res.* **70**, 1587 (1965); E. J. Smith, L. Davis, Jr., P. J. Coleman, Jr., C. P. Sonnett, *Science* **139**, 909 (1963); *J. Geophys. Res.* **70**, 1571 (1965); C. P. Sonett, *Space Sci. Rev.* **2**, 751 (1963).
2. S. S. Dolginov, Y. G. Yeroshenko, L. N. Zhuzgov, *Kosmich. Issled.* **6**, 561 (1968); K. I. Gringauz, V. V. Bezrukikh, L. S. Musatov, T. K. Breus, *ibid.*, p. 411; S. S. Dolginov, Y. G. Yeroshenko, L. Davis, *ibid.* **7**, 747 (1969).
3. H. S. Bridge, A. J. Lazarus, C. W. Snyder, E. J. Smith, L. Davis, Jr., P. J. Coleman, Jr., D. E. Jones, *Science* **158**, 1669 (1967); E. W. Greenstadt, *Cosmic Electrodyn.* **1**, 380 (1971).
4. K. I. Gringauz, V. V. Bezrukikh, G. I. Volkov, L. S. Musatov, T. K. Breus, *Kosmich. Issled.* **8**, 431 (1970).
5. N. F. Ness, K. W. Behannon, R. P. Lepping, K. H. Schatten, *J. Geophys. Res.* **76**, 3564 (1971); L. Davis, Jr., E. J. Smith, D. E. Jones, *ibid.* **78**, 4803 (1973); N. F. Ness, K. W. Behannon, R. P. Lepping, F. M. Neubauer, K. H. Schatten, *ibid.* **78**, 4809 (1973).
6. P. A. Cloutier, M. B. McElroy, F. C. Michel, *J. Geophys. Res.* **74**, 6215 (1969); R. Elco, *ibid.*, p. 5073; P. A. Cloutier, *Radio Sci.* **5**, 387 (1970).
7. J. R. Spreiter, A. L. Summers, A. W. Rizzi, *Planet. Space Sci.* **18**, 1281 (1970); A. W. Rizzi, thesis, Stanford University (1971) and references cited therein.
8. A. J. Dessler, in *The Atmospheres of Venus and Mars*, J. C. Brandt and M. B. McElroy, Eds. (Gordon & Breach, New York, 1968), p. 241; F. S. Johnson and J. E. Midgeley, *Space Res.* **9**, 760 (1969); F. C. Michel, *Rev. Geophys. Space Sci.* **9**, 427 (1971); J. L. Blank and W. R. Sill, *Bellcomm. TM 72-2015-1* (1972); P. A. Cloutier and R. E. Daniell, *Planet. Space Sci.* **21**, 463 (1973).
9. M. Wallis, *Cosmic Electrodyn.* **3**, 45 (1972); *Planet. Space Sci.* **21**, 1647 (1973).
10. E. W. Greenstadt, I. M. Green, G. T. Inouye, D. S. Colburn, J. H. Binsack, E. F. Lyon, *Cosmic Electrodyn.* **1**, 160 (1970); *ibid.*, p. 279; *ibid.*, p. 316; E. W. Greenstadt, *J. Geophys. Res.* **77**, 1729 (1972); *ibid.*, p. 5467; T. G. Northrop and T. J. Birmingham, *ibid.* **78**, 2308 (1973).
11. J. P. Heppner, M. Sugiura, T. L. Skillman, B. G. Ledley, M. Campbell, *J. Geophys. Res.* **72**, 5417 (1967); D. H. Fairfield, *ibid.* **74**, 3541 (1969); *ibid.*, in press; C. T. Russell, D. D. Childers, P. J. Coleman, Jr., *ibid.* **76**, 845 (1971); C. S. Wu, *ibid.* **77**, 575 (1972); A. Hasegawa, *ibid.* **77**, 84 (1972).
12. We thank our GSFC colleagues H. Burdick, R. Hoffman, D. Howell, F. Ottens, J. Scheifele, and J. Seek for their outstanding contributions to the success of this experiment; D. Fairfield, H. Völk, and the Mariner 10 plasma experiment team for beneficial discussions of results; and J. Bruns and G. Trusk of the Boeing Company and J. Dunne and W. E. Giberson and their staff at the Jet Propulsion Laboratory for contributions to the successful conduct of this study.

4 March 1974